World Academy of Science, Engineering and Technology
International Journal of Physical and Mathematical Sciences
Vol:6, No:9, 2012

Silicon-Waveguide based Silicide Schottky-Barrier Infrared Detector for on-Chip Applications

Shiyang Zhu, Guo-Qiang Lo, Dim-Lee Kwong

***Abstract*—**We prove detailed analysis of a waveguide-based Schottky barrier photodetector (SBPD) where a thin silicide film is put on the top of a silicon-on-insulator (SOI) channel waveguide to absorb light propagating along the waveguide. Taking both the confinement factor of light absorption and the wall scanning induced gain of the photoexcited carriers into account, an optimized silicide thickness is extracted to maximize the effective gain, thereby the responsivity. For typical lengths of the thin silicide film (10–20 μm), the optimized thickness is estimated to be in the range of 1–2 nm, and only about 50–80% light power is absorbed to reach the maximum responsivity. Resonant waveguide-based SBPDs are proposed, which consist of a microloop, microdisc, or microring waveguide structure to allow light multiply propagating along the circular Si waveguide beneath the thin silicide film. Simulation results suggest that such resonant waveguide-based SBPDs have much higher repsonsivity at the resonant wavelengths as compared to the straight waveguide-based detectors. Some experimental results about Si waveguide-based SBPD are also reported.

***Keywords*—**Infrared detector, Schottky-barrier, Silicon-waveguide, Silicon photonics

I. Introduction

One of the key components of Si photonics is the integrated photodetector (PD) sensitive to the long-haul communication wavelengths (1.30, 1.55 μm). Germanium/ silicon heterostructures have been commonly considered due to its low direct bandgap energy (~0.8 eV) [1]. However, epitaxial growth of high-quality Ge on Si imposes tremendous challenge on its integration scheme due to its defect-prone Ge-epi from lattice-mismatch and different thermal budget allowance on the existing Si-CMOS processing. Another approach is the incorporation of optical dopants (e.g., Er) [2] or defects with mid-bandgap energy states (e.g., induced by high-energy Si implantation) [3] into the silicon lattice. But these methods are also not the standard Si-CMOS processes. Silicide Schottky barrier photodiode (SBPD) is the third candidate, which is based on the photoexcitation of metal charge carriers across the silicide/Si interface and the cut-off wavelength is mainly determined by the Schottky barrier height (Φ_b) [4].

For operation at 1.30 or 1.55 μm, the conventional silicides used in the standard CMOS technology, i.e., Ti, Co and Ni silicides, can be adopted because they have Φ_b of 0.5–0.7 eV, thereby the corresponding cut-off wavelength of 1.8–2.4 μm.

Therefore, the SBPDs are completely compatible with the standard Si-CMOS processing with no new material addition and few processing modifications. Moreover, the speed of SBPDs is inherently faster than the conventional p-i-n PDs. The performance of SBPDs is primarily limited by the low responsivity because only a small fraction of photoexcited carriers in the silicide layer can emit through the silicide/Si interface to be collected as a photocurrent. The internal quantum yield is low of the order of 10^{-3} as calculated by the Fowler model [5]. The yield can be significantly enhanced, namely get a gain, if the silicide film is thin enough so that the photoexcited carriers moving away from the interface can be reflected to the emission barrier by wall or phonon scattering. However, the number of absorbed photons decreases dramatically with decreasing the silicide thickness. This conflict can be solved by using the waveguide configuration because the light is absorbed along the waveguide so that the silicide film on the waveguide can be lengthened unrestrictedly while keeping its thickness sufficiently thin. Such SOI waveguide-based SBPDs using ultrathin epitaxial $NiSi_2$ film as the absorption layer were recently demonstrated with encouraging performance [6], indicating the feasibility of waveguide-based silicide SBPDs.

Although theoretical analysis for the optical absorption in various silicides [7-9] and transport and emission of photoexcited carriers in the thin silicide films [4,10] have been intensively studied over the last several decades, the detailed analysis of the waveguide-based silicide SBPDs is still lack. In this paper, the optical absorption of silicide films on SOI channel waveguide is calculated using the RSoft simulator and some guidelines to optimize the silicide SBPDs are highlighted.

II. Optical absorption in the waveguide SBPDs

The complex index of refraction (n – *i*k) for various silicides is wavelength-dependent. For simplicity, we fix the wavelength at 1.55 μm in this study. Table 1 lists the n and k values of $NiSi_2$, NiSi, $CoSi_2$, and PtSi reported in literature [7-9]. The absorption coefficient (α) is calculated using RSoft BeamPROP.

As shown in inset of Fig. 1(a), the light power (P1) in Si (n = 3.4, k = 0) layer decays to be P2 in the SiO_2 layer (n = 1.45, k = 0) after propagating through a silicide film with thickness

This work was supported by the Science and Engineering Research Council of A*STAR Singapore under SERC grant number: 092 154 0098.

The authors are with the Institute of Microelectronics, Agency for Science, Technology and Research, 117685 Singapore (phone: 65-6770-5746; fax: 65-6773-1914; e-mail: zhusy@ime.a-star.edu.sg; logq@ime.a-star.edu.sg; kwongdl@ime.a-star.edu.sg).

TABLE I
OPTICAL PROPERTIES OF VARIOUS SILICIDE SCHOTTKY BARRIER PHOTODETECTORS AT 1550 NM

Property	Silicide			
	$NiSi_2$	NiSi	$CoSi_2$	PtSi
n	2.5	1.5	1.35	3.09
k	5.2	0.487	0.1915	1.08
α (μm^{-1})	43.76	23.02	31.75	44.17
Γ_0	1.47×10^{-2}	2.26×10^{-2}	7.79×10^{-3}	2.39×10^{-2}
d_0 (nm)	9.46	11.9	5.86	17.4
T_{opt} (nm)	2.0	1.8	2.1	2.3

The n and k values are cited from Refs [7-9].

The Γ_0 and d_0 values are extracted based on Eq. (3), for the structure of 0.56 μm wide silicide film on 0.2 μm × 1 μm straight Si channel waveguide.

T_{opt} is the optimized silicide thickness at the typical length of 10 μm calculated based on Eq. (6).

of d as:

$$P2/P1 = 1 - absorption = \exp(-\alpha \cdot d) \qquad (1)$$

The extracted α values for various silicides are listed in Table 1, which are close to the experimental data reported in literature [4,11].

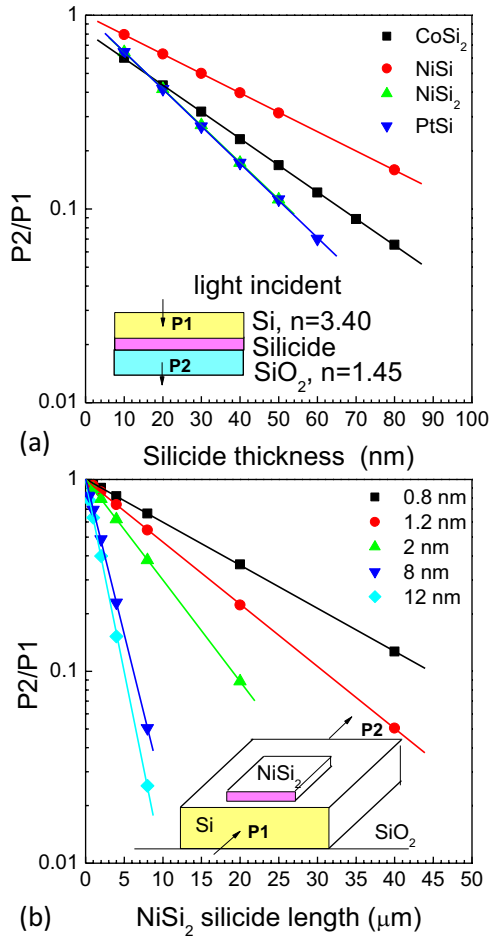

Fig. 1 Rsoft calculated optical absorption for (a) light propagating from a Si layer (light power P1) to a SiO_2 layer (light power P2) through a silicide layer; (b) light propagating though a 0.2 μm high and 1 μm wide SOI waveguide with a thin 0.56 μm wide $NiSi_2$ film on the top of the Si waveguide

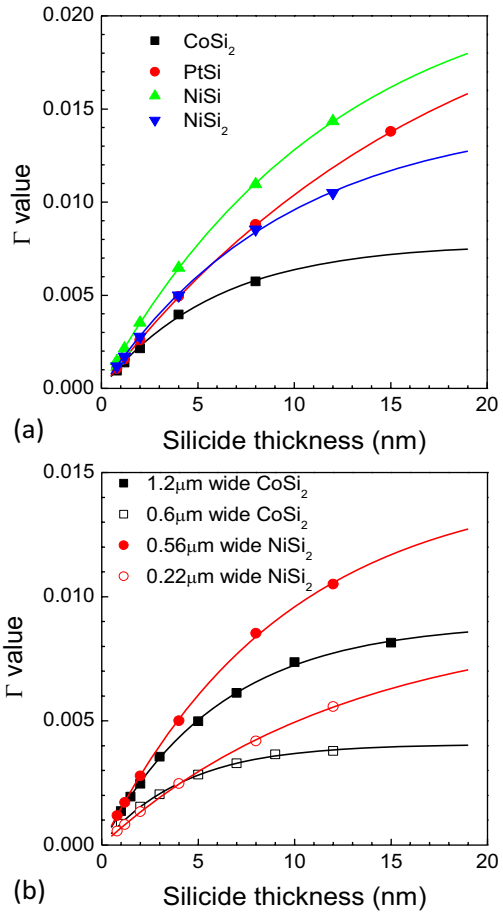

Fig. 2 The calculated confinement factor (Γ) as a function of the silicide thickness: (a) for 0.56 μm wide silicide film on a 0.2 μm × 1 μm Si waveguide; (b) for 0.6 and 1.2 μm-wide $CoSi_2$ on a 0.2 μm × 1.6 μm Si waveguide, and 0.22 and 0.56 μm-wide $NiSi_2$ on a 0.2 μm × 1 μm Si waveguide. The solid lines are fitting curves based on Eq. (3)

In the waveguide-based SBPDs, the silicide film is normally put on the straight Si waveguide and the structure is totally surrounded by the SiO_2 cladding layer, as schematically shown in inset of Fig. 1(b). The light power loss in the waveguide beneath a silicide layer is calculated using the RSoft BeamPROP modesolver. One example result is shown in Fig. 1(b) where the Si waveguide is set to be 0.2 μm (height) × 1 μm (width) and the $NiSi_2$ film with the width of 0.56 μm and thickness of 0.8–12 nm is put on the center of waveguide. The ratio of P2 (the light power in the waveguide after propagating through the silicide region with length of L) and P1 (the light power before the silicide region) can be expressed as:

$$P2/P1 = 1 - absorption = \exp(-\Gamma \cdot \alpha \cdot L) \qquad (2)$$

where Γ is the confinement factor. Fig. 2(a) shows the extracted Γ values as a function of silicide thickness for various silicides, where the geometry of the SOI waveguide and the silicide film is set to be the same as that of Fig. 1(b). The Γ value is found to depend on d as follows:

$$\Gamma(d) = \Gamma_0 \cdot \left(1 - \exp(-d/d_0)\right) \quad (3)$$

where Γ_0 and d_0 are factors, depending on both n and k of the silicide film. The extracted values of Γ_0 and d_0 are listed in Table 1 for various silicides. Fig. 2(b) shows the Γ value for different waveguide and silicide geometries. Eq. (3) is still valid, whereas both Γ_0 and d_0 decrease with decreasing the silicide width in respect to the waveguide width, in agreement to the fact that larger silicide film causes larger optical absorption.

III. Silicide Thickness Optimization for Waveguide SBPDs

The transport and emission of photoexcited carriers in thin silicide films have been intensively studied and several theoretical models exist in literature. Taking the phonon and wall scattering into account, Vickers expressed the internal quantum yield for uniform absorption and lossless phonon-electron collisions as [12]:

$$Y_V = \frac{(h\nu - \Phi_b)^2}{8E_f h\nu}(L_e/d)\cdot U(d/L^*) \quad (4)$$

where $h\nu$ is the photo energy, E_f is the silicide Fermi energy, L_e is the mean free path for collision with a cold electron, and $1/L^* = 1/L_e + 1/L_p$, where L_p is the mean free path for other bulk collision. The first term in Eq. (4) is the modified Fowler yield which describes the ratio of the number of collected charge carriers in Si to the number of excited charge carriers in the silicide, and is valid when $E_f >> h\nu$ and $h\nu > \Phi_b$. The product of the last two terms is the phonon and wall scattering induced enhancement. $U(d/L^*) \approx \left[1 - \exp(-d/L^*)\right]^{1/2}$ to within 10 percent for $d/L^* \geq 0.20$ [12]. Taking the optical absorption into account, the overall quantum efficiency or yield of the waveguide-based SBPDs can be expressed as:

$$Y = \left[1 - \exp(-\Gamma \cdot \alpha \cdot L)\right] \cdot Y_{opt} \cdot \frac{(h\nu - \Phi)^2}{8E_f h\nu} \cdot (L_e/d) \cdot \left[1 - \exp(-d/L^*)\right]^{1/2} \quad (5)$$

where Y_{opt} is the optical yield, defined as the ratio of the number of excited charge carriers in the silicide film to the number of absorbed photons. Both Y_{opt} and the modified Fowler yield are mainly determined by the slicide property, such as n, k, Φ_b, and E_f, rather than the silicide and waveguide geometries. Therefore, we may define the size-dependent effective gain as:

$$G_{eff} = \left[1 - \exp(-\Gamma(d) \cdot \alpha \cdot L)\right] \cdot (L_e/d) \cdot \left[1 - \exp(-d/L^*)\right]^{1/2} \quad (6)$$

When the silicide is selected, its length and thickness in the waveguide SBPDs can be optimized based on Eqs. (3) and (6) to reach the maximum G_{eff}.

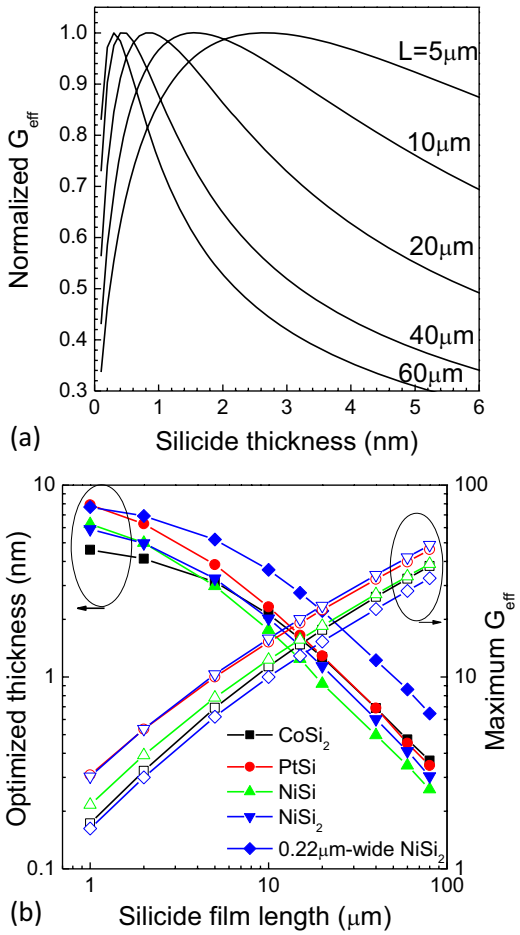

Fig. 3 (a) The normalized effective gain calculated using Eq. (6) as a function of the $NiSi_2$ film thickness; (b) the optimized silicide thickness (left axis)) and corresponding maximum G_{eff} (right axis) as a function of silicide film length for SBPDs with a 0.56 μm-wide silicide film on a 0.2 μm × 1 μm Si waveguide

However, both L_e and L_p depend on the silicide properties and their accurate values are not available. In literature, the values were reported within the range of $L_e \approx$ 50–500 nm and $L_p \approx$ 5–50 nm [10]. For simplicity, we just assume L_e = 100 nm and L_p = 10 nm in the following calculation. Fig. 3(a) plots the normalized G_{eff} as a function of silicide thickness at various silicide lengths for the 0.56-μm-width $NiSi_2$ silicide film on the 0.2 μm × 1 μm Si waveguide. We can see that there exists an optimized thickness at which the G_{eff} value reaches maximum. Fig. 3(b) plots the optimized thickness and corresponding maximum G_{eff} as a function of L for various silicides. The optimized thickness decreases and the corresponding G_{eff} increases as the silicide film length increasing. This result is obvious because thinner silicide film can get higher gain. For typical silicide film lengths of 10–20 μm in the waveguide-based SBPDs, the optimized thickness is only about 1–2 nm for various silicides. The estimated value is not sensitive to the L_e and L_p values, and should be even smaller if the optical absorption in the silicide/Si interface states is taken into account. Therefore, one key issue of the waveguide-based SBPDs is the fabrication of high-quality ultrathin silicide films.

However, the large sheet resistance of thin (e.g. <1 nm) and long (e.g. >10 μm) silicide films may degrade the detector's speed. It is a challenge to further improve the SBPD's reponsivity without sacrificing its speed.

The light propagating through a waveguide beneath the silicide film with certain length and corresponding optimized thickness is only partly absorbed. The absorption ratio, i.e., (1 – exp(−ΓαL)) is depicted in Fig. 4(a) as a function of L.

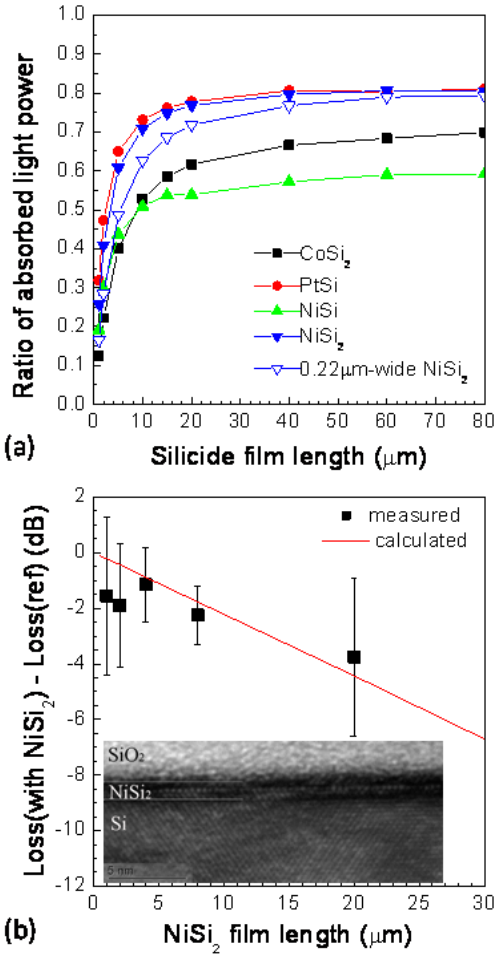

Fig. 4 (a) The ratio of absorbed light power through a waveguide beneath a silicide film with optimized thickness as a function of the silicide film length, the Si waveguide is 0.2 μm × 1 μm and the silicide width is 0.56 μm; and (b) The measured silicide induced optical loss as a function of the $NiSi_2$ film length where 0.56 μm wide $NiSi_2$ was epitaxially grown on a 0.2 μm high, 1 μm wide and 5.5 mm long SOI waveguide. The solid line is the calculated loss induced by a 0.8 nm thick $NiSi_2$ film. Inset shows the cross sectional TEM of the $NiSi_2$ film with the thickness of ~1.2 nm

We can see that the ratio of absorbed power increases quickly for L increasing from 1 μm to ~10 μm, and then saturates at about 50–80% for various silicides. This behavior is useful for the in-line PDs, but seems less efficiency for the terminal PDs. The optical absorption of ultrathin $NiSi_2$ films on the SOI waveguide was experimentally measured. The channel SOI waveguide has height of ~0.2 μm, width of ~1 μm, and length of ~5.5 mm and the silicide film on the waveguide has width of ~0.2 μm and length of 1–20 μm.

The ultrathin $NiSi_2$ films were formed by Ti-interlayer mediated epitaxy (TIME). XTEM image as shown in the inset of Fig. 4(b) indicates that the $NiSi_2$ film is epitaxial and has atomic flat interface on Si. The $NiSi_2$ film thickness is about 1.2 nm. SBPDs with such an ultrathin $NiSi_2$ have been demonstrated to have inspiring performance [6].

The silicide film induced optical loss was measured using a fiber–waveguide–fiber coupling system and one waveguide without silicide was used as a reference. The result is shown in Fig. 4 as a function of silicide film length. For comparison, the calculated curve for 0.8 nm thick NiSi2 film is also shown. Because the coupling loss between fiber and waveguide (~ 6 dB) is much larger than that induced by the ultrathin silicide film, the experimental data exhibit large error bar. Nevertheless, we can see that the light absorption of the unltrathin $NiSi_2$ film on the straight Si waveguide is quite small. It indicates that the responsivity reported in ref. [6] can be further improved if the light power can be substantially absorbed while keeping the film's thickness and length unchanged.

IV. Responsivity Enhancement using Resonant Structures

One obvious approach to improve the absorption of waveguide SBPDs without increasing the silicide thickness and length is to use a microloop structure [13] as schematically shown in Fig. 5(a), in which the light propagating one turn around the circular waveguide couples into the straight waveguide again by a Y-junction. The constructive interference occurs if $(2n_{Si}\pi/\lambda)\cdot(2\pi R) = 2k\pi$, where R is the circle radius and k is an integer. Therefore, such a microloop waveguide-based PD is wavelength-selective.

For a 0.2 μm × 1 μm channel waveguide, Fig. 6(a) depicts the light power at the circular waveguide region and that at the straight waveguide region as a function of R calculated using the RSoft FullWAVE simulator. The light power at the circular waveguide region is significantly enhanced at some specific radiuses. For small size channel waveguide-based SBPDs, the ultrathin silicide film can be put on the circle waveguide and the electrodes can be arranged as schematically shown in Fig. 5(b) to minimize its effect on the optical property of the microloop structure. For rib waveguide, the electrodes can be arranged at the side of waveguide. The microdisc structure shown in Fig. 5(c) can also be used to improve the responsivity. Fig. 6(b) compares the calculated light powers at the disc region and at the straight waveguide region as a function of the disc radius. In this structure, the electrode can be fabricated within the disc to save the chip area. However, its light energy enhancement is slightly lower than that of the microloop structure due to the larger loss of the microdisc structure as compared to the microloop structure. The above two structures use a Y-junction to combine the straight and circular waveguides, which results in ~3 dB coupling loss [14] for every turn of light propagating around the loop or disc. The microring structure shown in Fig. 5(c) can alleviate such a coupling loss, in which the ring lies adjacent to the straight waveguide.

Such a ring structure has been widely used as multiplexing and demultiplexing filters as well as the ring modulators. The microring waveguide-based SBPDs should have even higher responsivity as compared to the microloop and microdisc waveguide-based ones, but more processing difficulties associated with fabricating the precisely coupled microrings.

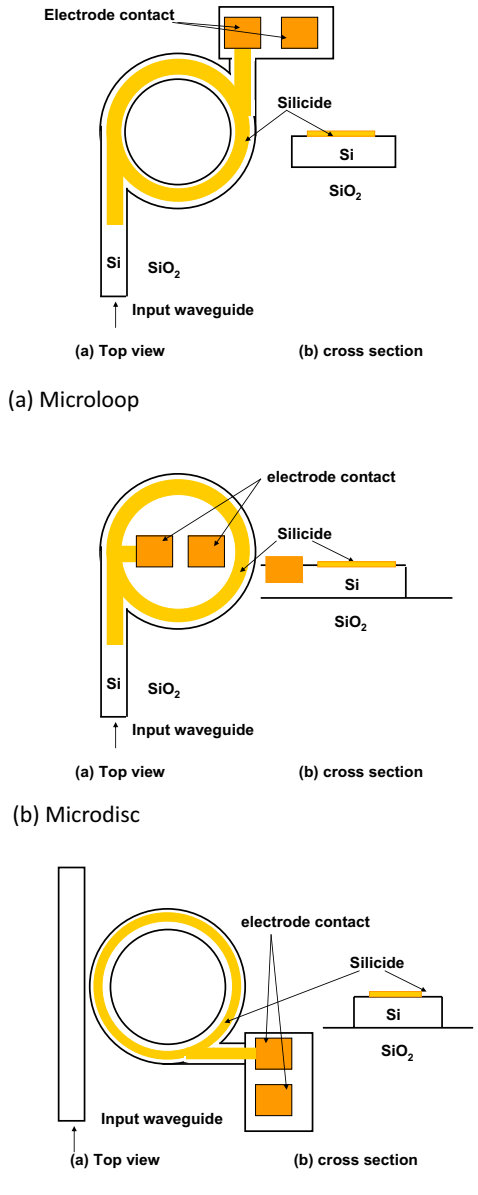

Fig. 5 Schematic top and side views of resonant channel waveguide-based SBPDs with (a) microloop; (b) microdisc; and (c) microring structure, the ultrathin silicide film is put on the circular waveguide and the possible electrode arrangement in various structures is also shown

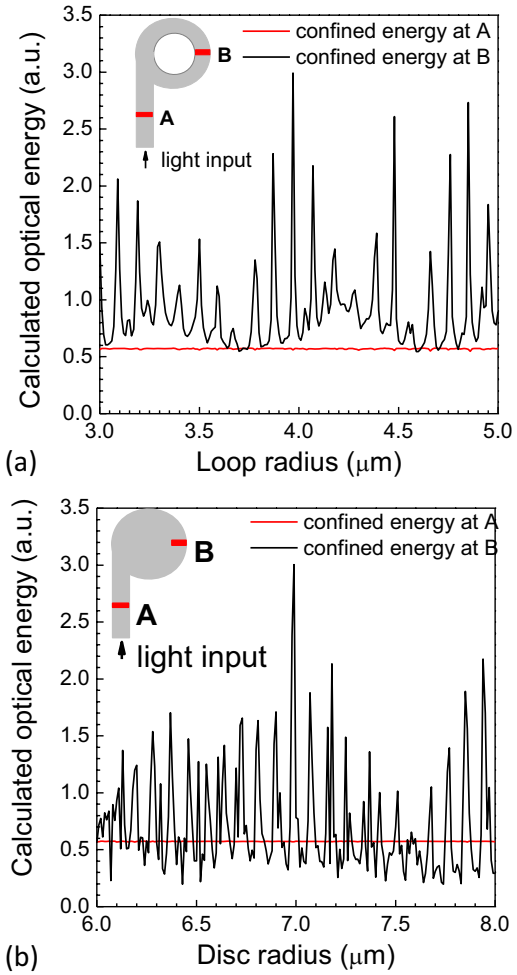

Fig. 6 The confined energy at the circular and straight waveguide regions in (a) microloop structure and (b) microdisc structure as a function of the radius calculated by the RSoft FullWAVE simulator, the channel Si waveguide size is 0.2 μm × 1 μm and the input light wavelength is 1.55 μm

V. Experimental Demonstration

The Si strip waveguide based SBPD is fabricated using standard CMOS technology. The layout of the device is shown in Figs. 7(a) and (b) schematically, which has a metal-semiconductor-metal configuration. After SiO_2 windows opening, ~1 nm Ti and ~5 nm Ni were sequentially deposited in a sputtering system, followed by rapid thermal annealing at 480°C for 30 s for silicidation, and the selectively wet etching to remove the unreacted metal. Such well-known self-aligned silicidation process can fabricate ultrathin smooth silicide film on Si. The fabricated devices are measured with 1550-nm light from a tunable laser source or a pulsed laser with 80-fs pulse width coupling into the Si channel waveguide through a lensed fiber. The measurement results of this detector are depicted in Fig. 8. The responsivity around 1550 nm is ~19 mA/W and the speed is ~7.0 GHz.

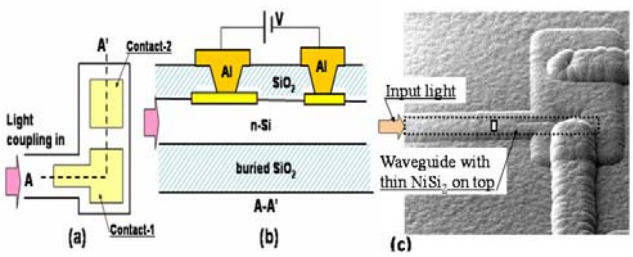

Fig. 7 (a) Schematic top view of silicon-on-insulator waveguide-based silicide Schottky-barrier MSM photodetector; (b) Schematic cross-sectional view of the detector; and (c) The SEM image of the fabricated detector

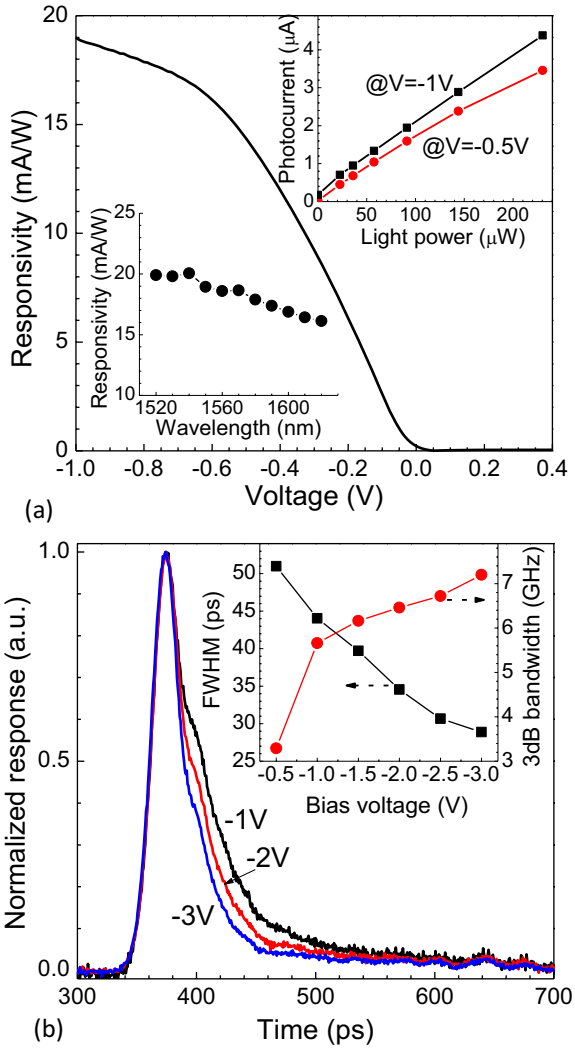

Fig. 8 (a) Responsivity of $NiSi_2$ MSM detector shown in Fig. 7 as a function of voltage, the top inset is the photocurrent versus the input light power, showing the almost linear response, the bottom inset is the responsivity versus wavelength in the range of 1520-1620 nm, showing that the responsivity decreases slightly with the wavelength increasing; (b) Normalized temporal response of the detector at -1, -2, and -3 bias under 1550-nm pulse illumination, the inset shows the FWHM and the 3-dB bandwidth obtained from Fourier transform of the temporal response

VI. Conclusion

The optical absorption for light propagating along a Si waveguide beneath a thin silicide film was calculated using the RSoft simulation. Taking both of the thickness-dependent confinement factor and the wall-scatting-induced gain into account, an optimized silicide thickness is extracted at which the effective gain thereby the responsivity of the straight waveguide-based SBPDs reaches the maximum. For typical silicide film lengths of ~10–20 μm, the optimized thickness is in the range of 1–2 nm for various silicides and only part power is absorbed to reach the maximum responsivity. Resonant waveguide-based SBPDs are proposed which consist of a microloop, microdisc, or microring structure and the unltrathin silicide film is put on the top of the circular waveguide. RSoft simulation indicates that such SBPDs are wavelength-sensitive and have significantly high responsivity owing to the resonant enhancement and effective absorption of the input light. The demonstrated detector already exhibits responsivity of ~19 mA/W and speed of ~7.0 GHz.

References

[1] S. J. Koester, J. D. Schaub, G. Dehlinger, and J. O. Chu, "Germanium-on-SOI infrared detectors for integrated photonic applications," *IEEE J. Sel. Topics Quantum Electron*, vol. 12, pp. 1489-1502, 2006.

[2] P. G. Kik, A. Polman, S. Libertino, and S. Coffa, "Design and performance of an erbium-doped silicon waveguide detector operating at 1.5 μm," *J. Lightwave Technol.*, vol. 20, pp. 834-839, 2002.

[3] J. B. D. Bradley, P. E. Jessop, and A. P. Knights, "Silicon-waveguide integrated optical power monitor with enhanced sensitivity at 1550 nm," *Appl. Phys. Lett.*, vol. 86, art. 241103, 2005.

[4] W. A. Cabanski and M. J. Schulz, "Electronic and IR-optical properties of silicide/silicon interfaces," *Infrared Phys.* vol. 32, pp. 29-44, 1991.

[5] R. H. Fowler, "The analysis of photoelectric sensitivity curves for clean metals at various temperatures," *Phys. Rev.*, vol. 38, pp. 45-56, 1931.

[6] S. Y. Zhu, M. B. Yu, G. Q. Lo, and D. L. Kwong, "Near-infrared waveguide-based nickel silicide Schottky-barrier photodetector for optical communications," *Appl. Phys. Lett.*, vol. 92, art. 081103, 2008.

[7] M. Amiotti, A. Borghesi, G. Guizzetti, and F. Nava, "Optical properties of polycrystalline nickel silicides," *Physical Review B*, vol. 42, pp. 8939-46, 1990.

[8] J. Y. Duboz, P. A. Badoz, J. Henz, and H. von Kanel, "Near-infrared optical properties of $CoSi_2$ thin films," *J. Appl. Phys.*, vol. 68, pp. 2346-2350, 1990.

[9] J. M. Mooney, "Infrared optical absorption of thin PtSi films between 1 and 6 μm." *J. Appl. Phys.*, vol. 64, pp. 4664-4667, 1988.

[10] J. Martin Mooney and J. Silverman, "The theory of hot-electron photoemission in Schottky-barrier IR detectors," *IEEE Trans. Electron Devices*, vol. 32, pp. 33-39, 1985.

[11] J. Kurianski, J. Van Damme, J. Vermeiren, K. Maex, and C. Claeys, "Nickel silicide Schottky barrier detectors for short wavelength infrared applications," *Proc. SPIE* ***1308*** *Infrared detectors and focal plane arrays*, pp. 27-35, 1990.

[12] V. E. Vickers, "Model of Schottky barrier hot-electron-mode photodetection," *Appl. Opt.*, vol. 10, pp. 2190-2192, 1971.

[13] G. Abaeiani, V. Ahmadi, and K. Saghafi, "Design and analysis of resonant cavity enhanced-waveguide photodetectors for microwave photonic applications," *IEEE Photonics Technology Lett.*, vol. 18, pp. 1597-1599, 2006.

[14] M. Lipson, "Guiding, modulating, and emitting light on silicon – challenges and opportunities," *J. Lightwave technology*, vol. **23**, pp. 4222-4238, 2005.